Solar Energetic Particle Events of July 2017: Multi-spacecraft Observations near 1 and 1.5 au

C. Krishnaprasad[1,2], Smitha V. Thampi[1], Christina O. Lee[3], Srikar P. Tadepalli[4], K. Sankarasubramanian[4], and Tarun K. Pant[1]

[1]Space Physics Laboratory, Vikram Sarabhai Space Centre, Thiruvananthapuram 695022, India
[2]Cochin University of Science and Technology, Kochi 682022, India
[3]Space Sciences Laboratory, University of California, Berkeley, CA 94720, USA
[4]U. R. Rao Satellite Centre, Bengaluru 560017, India

Key Points:

- Multi-spacecraft observations of solar events of late solar cycle 24 in July 2017 are presented. Observations near Earth, STEREO-A, and near Mars are used.
- Solar Energetic Particle (SEP) enhancement is observed at a remote observer location due to IMF connectivity with the CME shock elsewhere.
- Spectral analysis of the SEP events associated with CMEs and SIRs are carried out and the spectral features are interpreted in terms of acceleration, transport, and magnetic connectivity.

D R A F T Tuesday 23rd June, 2020, 15:21 IST

Corresponding author: C. Krishnaprasad, kpchirakkil@gmail.com

Abstract

We investigate the space weather events of late solar cycle 24 in July 2017 observed by a number of spacecraft in the inner heliosphere widely separated in heliolongitude and radial distance. These include spacecraft at L1 point, STEREO-A, near Earth satellites, and MAVEN (near Mars). The GRASP payload onboard Indian GSAT-19 satellite provides a new vantage point for Solar Energetic Particle (SEP) observations near Earth. There were two major Coronal Mass Ejections (CMEs) and one Stream Interaction Region (SIR) event in July 2017. The 16 July CME was Earth directed and the 25 July CME was STEREO-A and Mars directed. Earth and Mars were on the opposite sides of the solar disk, while Mars and STEREO-A were aligned with respect to the nominal Parker spiral field. The 25 July event was more stronger and wider in heliolongitude. This CME shock had magnetic connectivity to Earth, which produced an SEP event at Earth ∼two days later. The spectral indices of the event observed directly at STEREO-A and remotely at ACE was found to be similar. The 17 July SIR event was observed by both MAVEN and STEREO-A. Higher particle intensities (a factor of 6 enhancement for 1 MeV ions) are observed by MAVEN (at 1.58 au) compared to STEREO-A (at 0.96 au). Also a spectral hardening is observed while comparing the spectral indices at these two locations, indicating an acceleration of energetic ions in SIR shock during the radial propagation of 0.62 au in the interplanetary space.

1 Introduction

Solar Energetic Particles (SEPs) are the high energy protons, electrons, alpha particles, and heavy ions released from the Sun and accelerated at or near the Sun or in the heliosphere (e.g. recent reviews by Desai and Giacalone (2016); Klein and Dalla (2017)). These particles are of energies in the range tens of keV upto a few GeV. Solar flares, Coronal Mass Ejections (CMEs), and Corotating Interaction Regions (CIRs) are major sources of energetic particles in the inner heliosphere and these transients have severe impact on the atmosphere and ionosphere of unmagnetized planets, such as increased atmospheric loss at Mars (e.g. Krishnaprasad, Thampi, and Bhardwaj (2019); Lee et al. (2018); Thampi et al. (2018)). Parker (1958) first suggested that interplanetary magnetic field (IMF) lines form an Archimedean–spiral shape, if solar wind expansion were independent of time and heliolongitude (that is, a uniform radial expansion of solar wind). However this is not true when the solar wind is highly variable. The SEPs undergo changes in their properties, such as they accelerate at flare sites or at shocks upon traveling through the heliosphere. It is also observed that the energetic particle increases in intensity–time profiles have well–defined forms dependent on the location of the source relative to the observer and the presence and strength of interplanetary shocks (Cane, Reames, & von Rosenvinge, 1988; Reames, 1995; Van Hollebeke, Ma Sung, & McDonald, 1975). Based on the intensity rise rate and duration, SEP events are generally classified into 'gradual' and 'impulsive' (Reames, 2013).

The SEP events of July 2017 are special in a sense that these are quite intense and appeared in the late phase of the historically weak solar cycle 24 (Dumbović et al., 2019; Luhmann et al., 2018). This is surprising, as we do not expect such intense energetic particle events in the declining and late phase of a solar cycle. But such exceptional solar activity is not unprecedented and in fact the late solar cycle 23 also had such SEP events (von Rosenvinge et al., 2009). An enhancement in SEP flux is observed at a vantage point either when the shock associated with a stream or ejection directly passes the observer, or if the IMF is connected to the observer site (as the charged particles can gyrate and move along the field lines, i.e. parallel transport from the source to the observer), or because of perpendicular transport by cross–field diffusion or drift (Zhang, Qin, & Rassoul, 2009).

The particles released in CMEs are generally accelerated close to the Sun (∼3–10 solar radii, i.e. within 1 au), and are streamed out through the heliosphere following magnetic field lines (Chollet et al., 2010). These gradual events are observed over a wide longitude interval, unlike the impulsive events which are restricted to $< 30^\circ$ longitude cone (Reames,

1995). The intensity peak near the shock is generally called the Energetic Storm Particle (ESP) event. In large CME-related SEP events, changes in field line connectivity of the spacecraft to different particle acceleration regions will result in changes in intensity–time profiles. Recently, Xie, Mäkelä, St. Cyr, and Gopalswamy (2017) studied three SEP events observed in the solar cylce 23 by STEREO A, B, and near-Earth (L1) spacecraft with a wide longitudinal distribution of particles. They examined whether the observations of SEPs from different vantage points could be explained by acceleration and injection by the spatially extended shocks or whether another mechanism such as cross-field transport is required, and found that cross-field diffusion is the likely candidate for some of the enhancements observed with wide longitudinal spread. Simultaneous observations of SEP events using a constellation of spacecraft, at different longitudes and radial positions, may give us an idea of how the longitudinal spread of the SEP intensity varies, in addition to other observables.

The combination of observations performed simultaneously by several spacecrafts located at various heliospheric locations is a tool to investigate the spatial distribution of SEP events. Using measurements from widely separated spacecrafts in longitude and radial distance in the inner heliosphere, we examine SEP intensity–time profiles present in the July 2017 events and discuss their attributes in the context of the Sun, state of the surrounding heliosphere, in situ plasma and magnetic field signatures, spacecraft's magnetic connectivity to the shock, and the spectral differences at these locations.

2 Data and Method of Analysis

The observations from the first Sun–Earth Lagrange point (L1 at ∼0.99 au) are from the Electron Proton Alpha Monitor (EPAM) onboard the Advanced Composition Explorer (ACE) spacecraft (Gold et al., 1998). The observations near Earth are from the Energetic Particle Sensor (EPS) onboard Geostationary Operational Environmental Satellites (GOES-13), Geostationary Radiation Spectrometer (GRASP) onboard Geostationary Satellite (GSAT-19), and the Solid State Telescope (SST) onboard Acceleration Reconnection Turbulence and Electrodynamics of the Moon's Interaction with the Sun (ARTEMIS) spacecraft. The Solar TErrestrial RElations Observatory (STEREO-A) Solar Electron Proton Telescope (SEPT; Müller-Mellin et al. (2008)), Low Energy Telescope (LET; Mewaldt et al. (2008)), and High Energy Telescope (HET; Richardson et al. (2014); von Rosenvinge et al. (2008)) particle telescopes are also used for energetic particle observations at 1 au from a different heliospheric longitude with respect to near–Earth spacecraft. The solar wind plasma and IMF data at 1 au, as well as GOES-13 differential and integral fluxes are taken from OMNIWeb data center (`https://omniweb.gsfc.nasa.gov/`). The ACE SEP data are obtained from ACE Science Center (`http://www.srl.caltech.edu/ACE/ASC/`) and the STEREO-A SEP data are obtained from STEREO Science Center (`http://www.srl.caltech.edu/STEREO/`). The ARTEMIS SEP data are obtained from `http://artemis.ssl.berkeley.edu/`.

GSAT-19 is an Indian communication satellite launched in June 2017 that carries GRASP payload to monitor and study the nature of charged particles and the influence of space radiation on satellites and their electronic components. The instrument measures the energy and flux of incident particles, and also enables particle identification by the E–dE technique. GSAT-19 is orbiting in 82°E longitude, while GOES-13 was at 75°W longitude of Earth. The in situ measurements from GRASP can provide additional data from geostationary orbit that can lead to improved models on space radiation.

The Solar Energetic Particle (SEP) instrument onboard Mars Atmosphere and Volatile EvolutioN (MAVEN) spacecraft in orbit around Mars provides SEP ion and electron observations near 1.5 au (Larson et al., 2015). This instrument consists of two identical sensors, SEP1 and SEP2, each consisting of a pair of double-ended solid-state telescopes to measure 20 keV–200 keV electrons and 20 keV–6 MeV ions in four orthogonal view directions that are positioned to adequately cover the canonical Parker spiral direction around which SEP

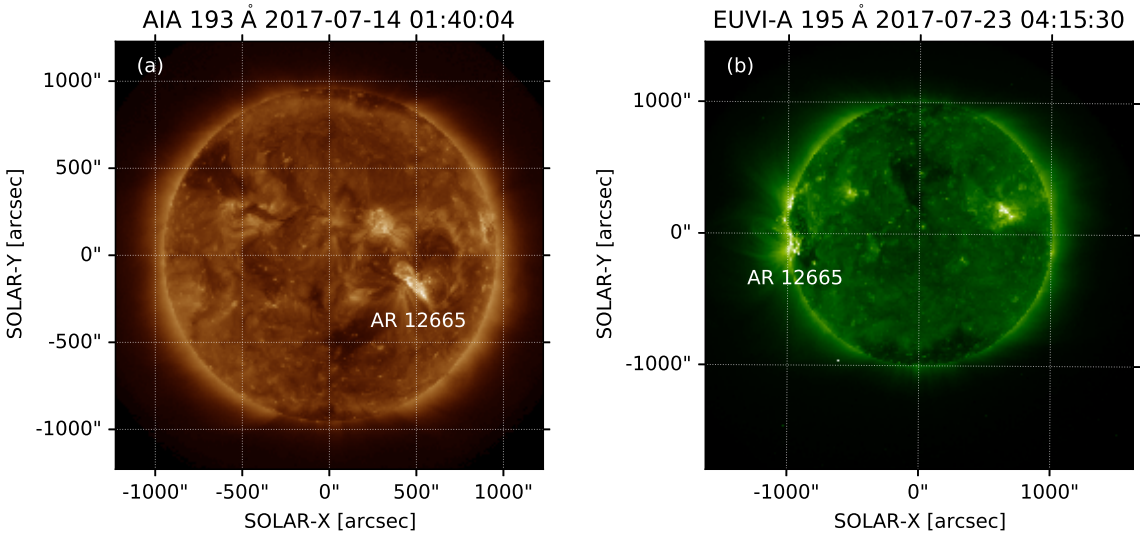

Figure 1. CME eruption site near AR 12665 on the solar disk imaged by (a) SDO/AIA on 14 July, 01:40 UT and (b) STEREO-A/EUVI on 23 July, 04:15 UT.

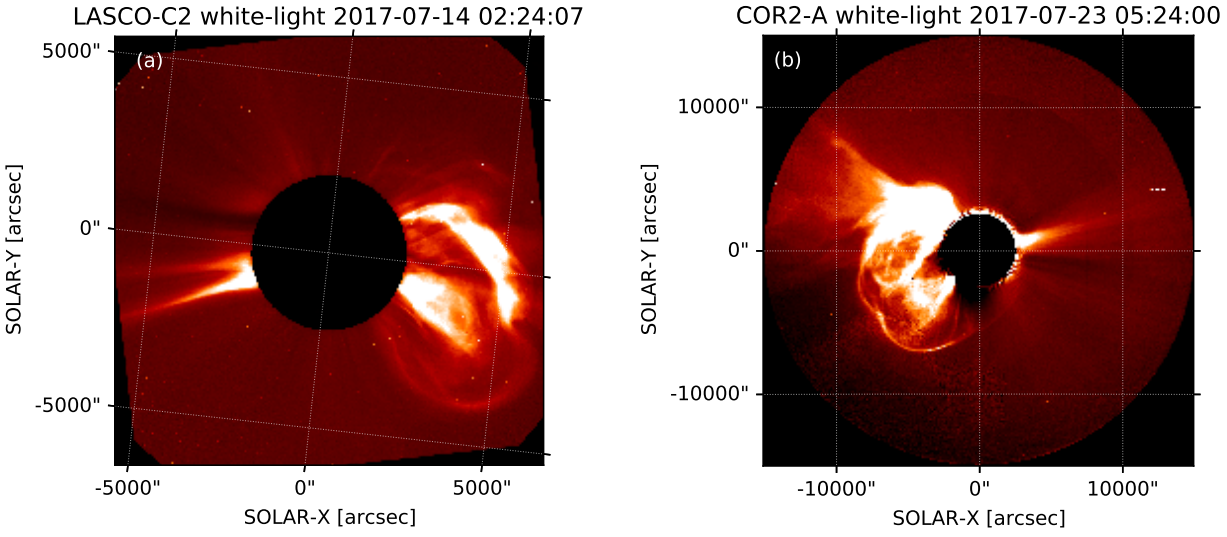

Figure 2. (a) CME structure on 14 July, 02:24 UT by SOHO/LASCO C2 and (b) CME structure on 23 July, 05:24 UT by STEREO-A/COR2.

distributions are centered (Larson et al., 2015). The data used in this study are the ion data in the form of energy fluxes measured by the SEP1 sensor in the forward and reverse looking FOVs. The ion counts measured by SEP/MAVEN in the lower energy channels (< 100 keV) are also contributed by the O^+ pickup ions from Mars, and hence are removed from the analysis (Larson et al., 2015; Rahmati et al., 2015). The MAVEN data are obtained from the Planetary Data System (`https://pds.nasa.gov/`).

During July 2017, both STEREO-A and Mars were located at the back side of the Sun as viewed from Earth. STEREO-A was at -132° HEE (Heliocentric Earth Ecliptic) longitude, and Mars was at $\sim$ -178° HEE longitude, with a longitudinal separation of $\sim$46° between STEREO-A and Mars (with Earth being at a reference heliolongitude of 0°). Mars was at a radial distance of 1.58 au from the Sun, while STEREO-A was at $\sim$0.96 au during this period.

The Wang-Sheeley-Arge (WSA)-ENLIL+Cone model simulations (Mays et al., 2015; Odstrcil, 2003) are taken from Community Coordinated Modeling Center (CCMC; `https://ccmc.gsfc.nasa.gov/`). This combined time-dependent model consists of solar coronal model WSA coupled with the global heliospheric solar wind magnetohydrodynamic (MHD) model ENLIL, and CMEs (spherical shaped high pressure gusts) inserted using Cone model–3D CME kinematic and geometric parameters. The inputs to the model simulations shown in Figures 1 and 2 (such as the National Solar Observatory (NSO) Global Oscillation Network Group (GONG) Potential Field Source Surface (PFSS) synoptic magnetic field maps and Cone model parameters) are described in Luhmann et al. (2018). The simulated solar wind velocities appear to capture the ACE and STEREO-A observed velocities, thus giving confidence on the wider inner heliospheric simulations (Luhmann et al., 2018).

3 Observations

There were two major CME eruptions during July 2017. The Active Region (AR) 12665 (located around S07W44) was the prominent eruptive region on the Sun during this period (Luhmann et al., 2018). The main eruptions for the period were multiple, with fast and wide ejections following one another by roughly a week with the CME ejecta headed first to the west of Earth and then later in the general direction of STEREO-A and Mars (Luhmann et al., 2018). Figure 1a shows the Solar Dynamics Observatory (SDO) Atmospheric Imaging Assembly (AIA) image of the solar disk, and Figure 1b shows the STEREO-A Extreme Ultraviolet Imager (EUVI) image of the solar disk. Both images indicate the presence of eruption site near the active region, as well as the presence of CME loops.

Figure 2 shows the CME structures observed by the white light coronagraphs onboard Solar and Heliospheric Observatory (SOHO) and STEREO-A during the two major interplanetary CME events of July. The SOHO/LASCO (Large Angle and Spectrometric Coronagraph) C2 coronagraph image (Figure 2a) and STEREO-A/COR2 coronagraph image (Figure 2b) show the CME eruptions.

Figure 3 shows the snapshots of WSA-ENLIL+Cone model simulations of inner heliospheric conditions such as solar wind radial velocity and IMF lines during 14 to 20 July 2017 event at Earth (hereafter 16 July event; Figure 3a) and 23 to 28 July 2017 event at STEREO-A and Mars (hereafter 25 July event; Figure 3b). The event period WSA-ENLIL+Cone simulation results for July are described in detail by Luhmann et al. (2018). The July 2017 events seemed to arise in conjunction with the appearance of a coronal psuedostreamer (Luhmann et al., 2018). The simulations show the magnetic field lines during the event period, and some of which connects between the spacecraft and the CME shocks inside as well as outside the spacecraft heliocentric radius. Luhmann et al. (2018) calculated the shock connection radius, which shows that Earth is connected to shocks from outside 1 au during the 26 July event.

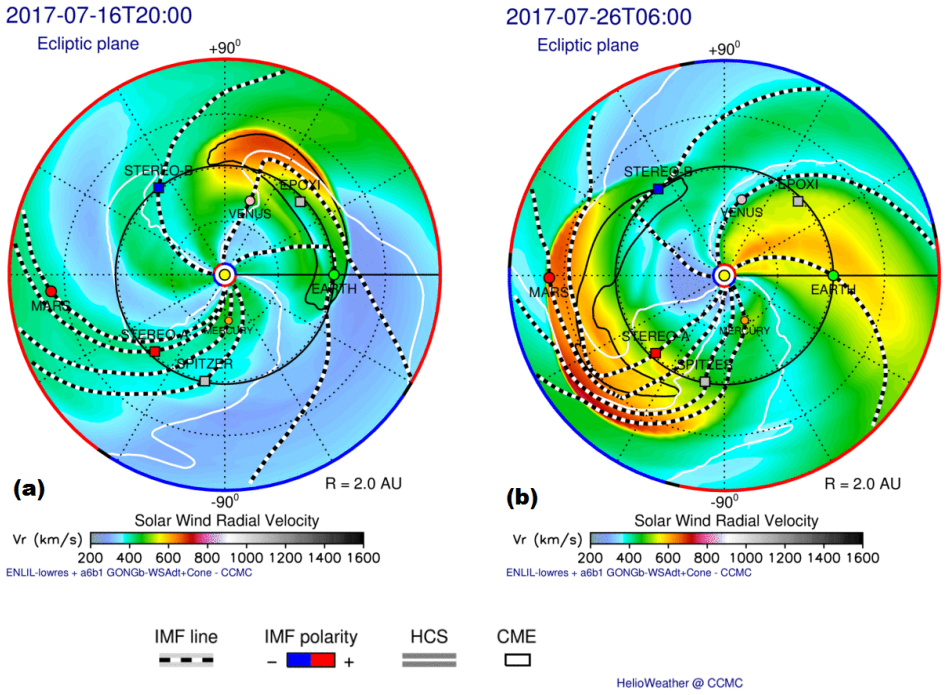

Figure 3. The snapshots of WSA-ENLIL+Cone model simulations of inner heliospheric conditions such as solar wind radial velocity (color contour) and IMF lines (black and white lines) during (a) 14 to 20 July 2017 event at Earth (the 16 July event) and (b) 23 to 28 July 2017 event at STEREO-A and Mars (the 25 July event).

The 16 July event observed at L1 point by ACE spacecraft and at Earth's geostationary orbit by GOES and GSAT-19 satellites was due to an Earth directed CME. Figure 4a shows the IMF and solar wind velocity observed by ACE during 12 to 31 July 2017. The interplanetary data are based on the OMNIWeb database, which provides in situ observations time-shifted to the bow shock nose of the Earth. A fluctuating IMF with increase in total $|B|$ to ∼25 nT and an increase in solar wind speed to 664 km sec^{-1} was observed. Figure 4b shows the SEP intensity–time profiles of energetic ions in different energy channels (between ∼100 keV and 4.75 MeV) observed by EPAM/ACE. The SEP intensities increase gradually from 14 July upto 20 July, with a crescendo observed on 16 July. The peak flux during this period in the lowest energy channel (110 keV to 190 keV) was 3×10^5 pfu MeV^{-1} (here the particle flux unit, 1 pfu = 1 particle cm^{-2} s^{-1} sr^{-1}). The sudden spikes in the intensity profiles, such as those seen on 22 July are due to the accelerated ions propagating from the Earth's bow shock (Bruno, Christian, de Nolfo, Richardson, & Ryan, 2019). The event was also observed by GOES and GSAT-19. The ion flux enhancement can be seen from 14 to 16 July with a peak enhancement of 12 pfu in GOES >10 MeV channel and 7 pfu in GSAT-19/GRASP 5-85 MeV channel (Figure 4c). This enhancement seen at GOES and GSAT is before the peak flux observed at ACE. This is because the GOES and GSAT detected ions are of higher energies, which travel faster than the comparatively low-energy SEPs observed by ACE. This event was also observed by the solid state telescopes onboard ARTEMIS P1 and P2 (the former THEMIS b and c satellites) in orbit around Moon. The observed intensity–time profiles of 100 keV to 6 MeV energetic ions are similar to the ACE observations (not illustrated).

The second major event of July, starting from 23 July and lasting upto 28 July is primarily due to a Mars directed CME, which was observed by both STEREO-A and MAVEN.

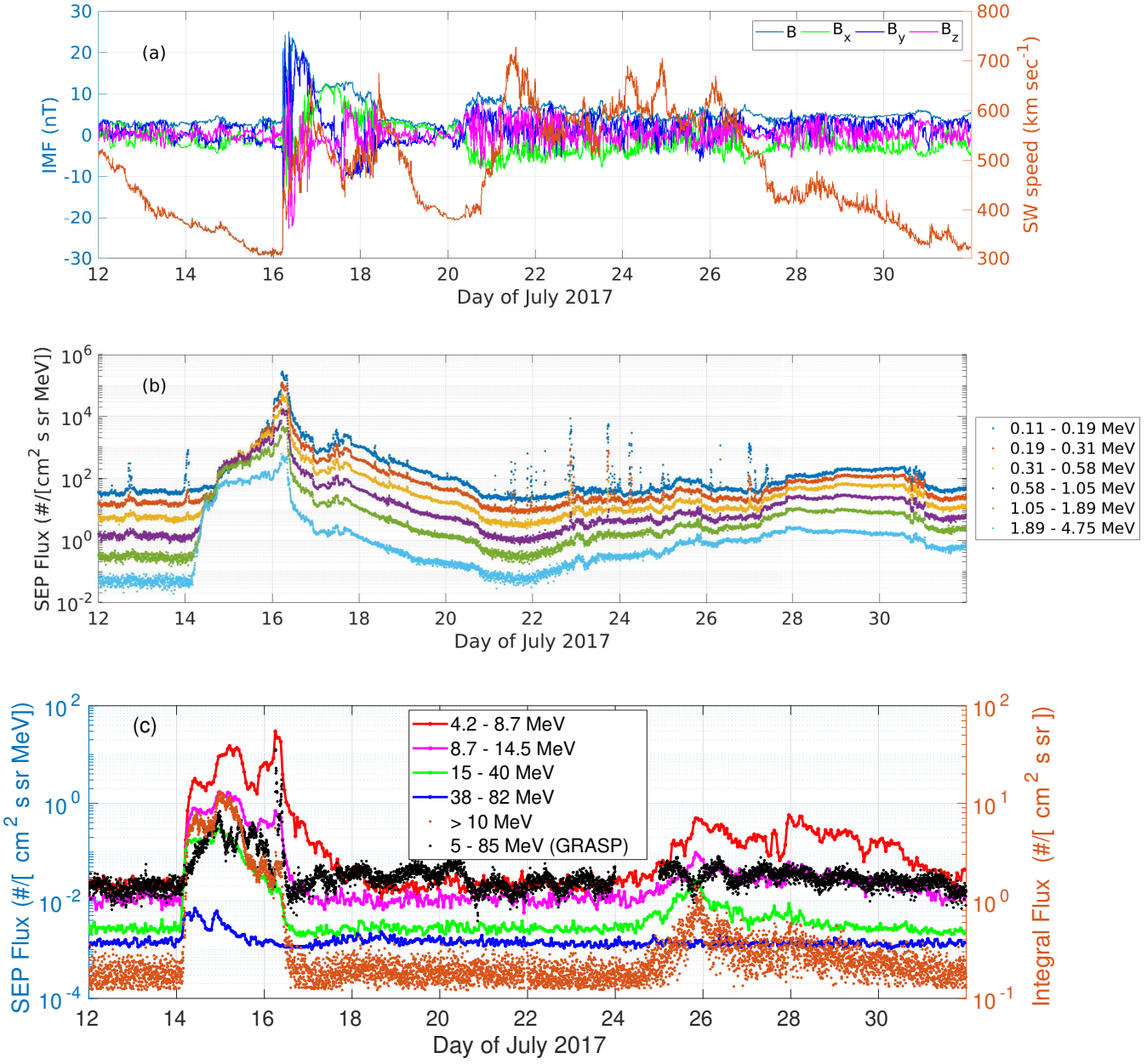

Figure 4. (a) The near Earth observations of IMF ($|B|$, B_x, B_y, B_z) and solar wind speed during 12–31 July 2017, (b) ACE observations of SEP intensity–time profiles during 12–31 July 2017, and (c) GOES observations of SEP intensity–time profiles (differential and integral fluxes) during 12–31 July 2017.

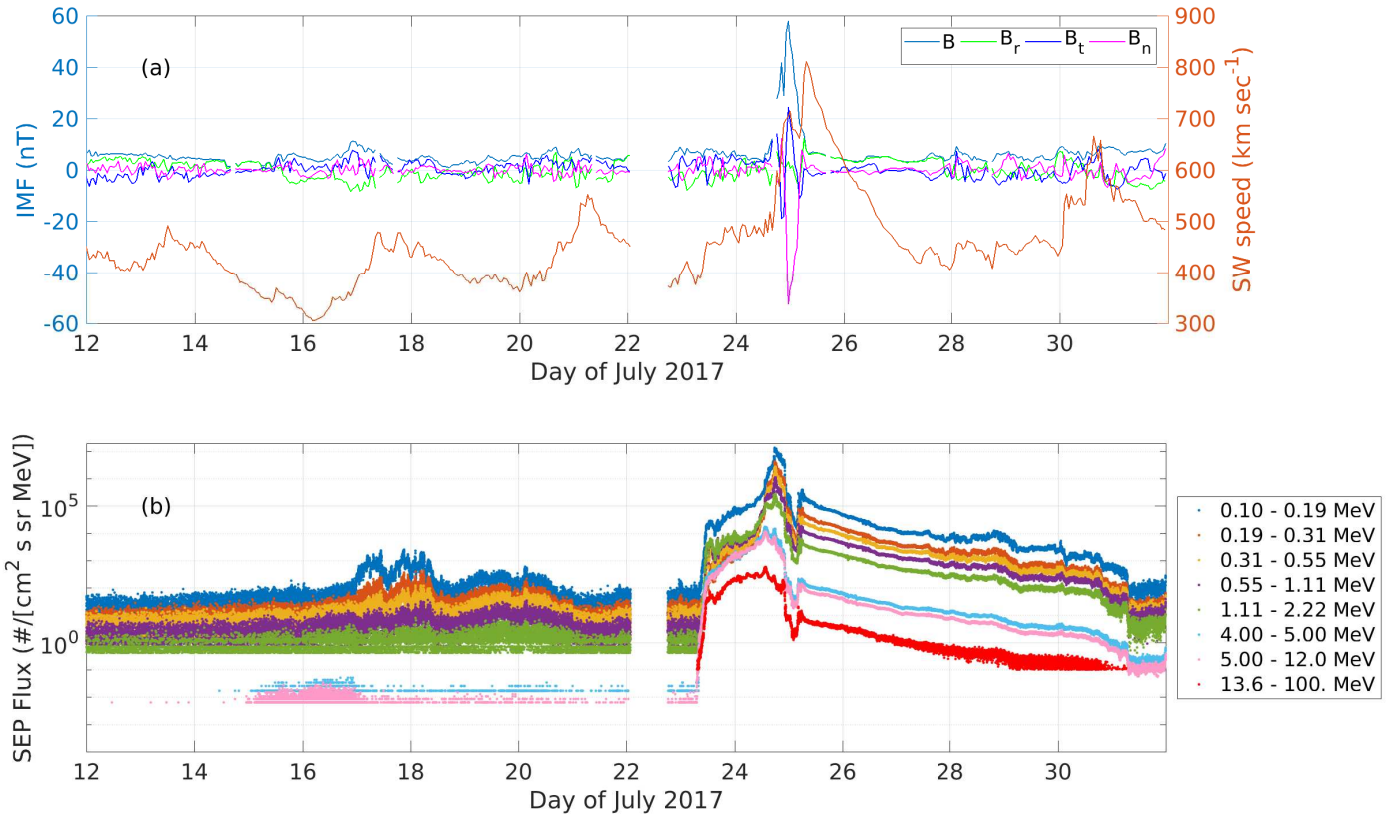

Figure 5. (a) The STEREO-A observations of IMF ($|B|$, B_r, B_t, B_n) and solar wind speed during 12–31 July 2017 and (b) STEREO-A (SEPT, LET, HET telescopes) observations of SEP intensity–time profiles during 12–31 July 2017. The white gap on 22 July is due to absence of data.

Figure 5a shows the IMF and solar wind velocity observed by STEREO-A during 12 to 31 July 2017. The peak total magnetic field was 58 nT (on 24 July) and peak solar wind speed was 811 km sec^{-1} (on 25 July). Figure 5b shows the SEP intensity–time profiles of energetic ions of energy between 100 keV and 100 MeV in different channels. The maximum enhancement seen in the lowest energy channel (100 keV to 190 keV) was $>10^7$ pfu MeV^{-1} on 24 July. The different energy channels shown in Figure 5b are from SEPT ($\sim$100 keV to 2.2 MeV), LET (4 to 12 MeV), and HET (>13 to 100 MeV) particle detectors onboard STEREO-A. The event was also observed by MAVEN in orbit around Mars. Figure 6a shows the upstream solar wind velocity and magnetic field measurements from MAVEN spacecraft. The upstream solar wind velocity from Solar Wind Ion Analyzer (SWIA) and IMF from Magnetometer (MAG) are obtained using the method given by Halekas et al. (2017). Figure 6b shows the energy–time spectrogram of differential energy flux of ions from 12 to 31 July observed by the forward facing sensor one (1F) of SEP instrument onboard MAVEN. An enhancement in SEP flux is observed between 23 and 28 July 2017. Figure 6c shows the intensity–time profiles of ions in different energy channels between 100 keV and 5.11 MeV by forward looking sensor (1F) and Figure 6d shows the observations by reverse looking sensor (1R). A peak flux of 2×10^5 pfu MeV^{-1} was observed on 26 July in the 100 keV to 200 keV energy channel. The data just prior to the peak of ion flux enhancement are removed because of electron contamination to the ion channels, in the vicinity of peak electron flux (Luhmann et al., 2018). The reverse facing data are also shown, because the pick-up oxygen ions predominantly appear in the forward facing MAVEN/SEP detectors and hardly appear in the reverse facing detectors, and therefore confirms the presence of SEP related enhancements (Larson et al., 2015).

SEP flux enhancements due to Stream Interaction Regions (SIRs) were also present during the period in July 2017. Two SIR events are identified from the solar wind and magnetic field data and STEREO IMPACT Level-3 solar events list (`https://stereo-ssc.nascom.nasa.gov/data/ins_data/impact/level3/`). One from 16 to 18 July (with a maximum solar wind speed of 493 km sec^{-1} and magnetic field intensity of 12.5 nT) and another one from 19 to 21 July (with a maximum solar wind speed of 572 km sec^{-1} and magnetic field intensity of 10.2 nT). The former (hereafter 17 July event) had higher SEP intensities compared to the latter (Figure 5b).

Interestingly, energetic particle enhancement is also observed (at Earth) when the CME was not directly passing the observer, and when the observer is on the opposite side of the Sun as viewed from the CME longitude. Energetic particle enhancements can be seen in ACE profiles (28-30 July, Figure 4b), as well as in GOES lower energy channels such as 4.2 to 8.7 MeV (Figure 4c). This is during the period when the 25 July event is hitting the STEREO-A and Mars, both spacecraft on the western heliospheric longitude. This SEP enhancement observed at Earth's location is due to magnetic connections to distant shocks, that is shocks beyond heliocentric radius of the observer (Figure 5a of Luhmann et al. (2018)). The SEPMOD calculations based on the ENLIL simulation results for similar proton energy range are capturing the smaller enhancements during 28-30 July (Luhmann et al., 2018). We can also see that bulk solar wind speed and IMF do not show any significant enhancement during 27 to 31 July when the SEP enhancement is observed at ACE location. However the solar wind speed is relatively higher for a period prior to the SEP enhancement from 21 to 26 July (Figure 4a). This could be due to the passage of a high speed stream during this period as observed from the ENLIL simulation shown in Figure 3b.

Figure 7a shows the power-law fits for SEP energy spectra during July 2017 events observed by ACE. The energy spectra are fitted with a power-law of the form $AE^{-\gamma}$. Two distinct SEP enhancements were detected by ACE from 14 to 20 July, associated with CME eruptions. The event averaged spectrum of the two SEP events are shown in red (14/07, 18:14 UT to 17/07, 00:43 UT) and brown (17/07, 15:50 UT to 20/07, 18:57 UT) colors. The event averaged spectrum of the SEP enhancement due to shock connectivity is shown in magenta color (27/07, 21:22 UT to 30/07, 15:50 UT).

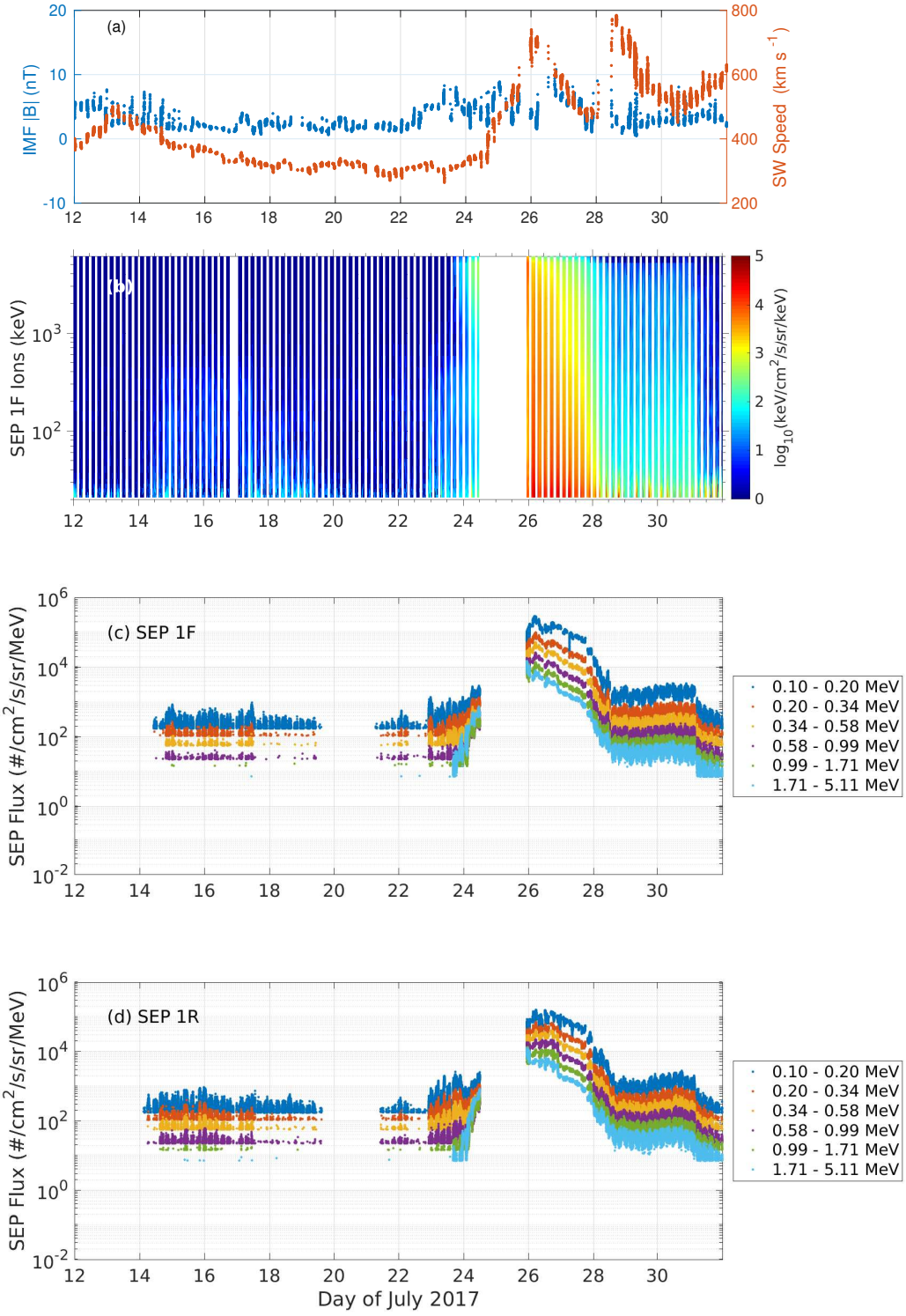

Figure 6. (a) The MAVEN (near Mars) upstream observations of IMF ($|B|$) and solar wind speed during 12–31 July 2017, (b) MAVEN observations of SEP energy–time spectrogram of differential energy flux during 12–31 July 2017, and (c) MAVEN observations of SEP intensity–time profiles during 12–31 July 2017. The white gap before 22 July is due to low flux of particles, while after 22 July is due to poor quality of data.

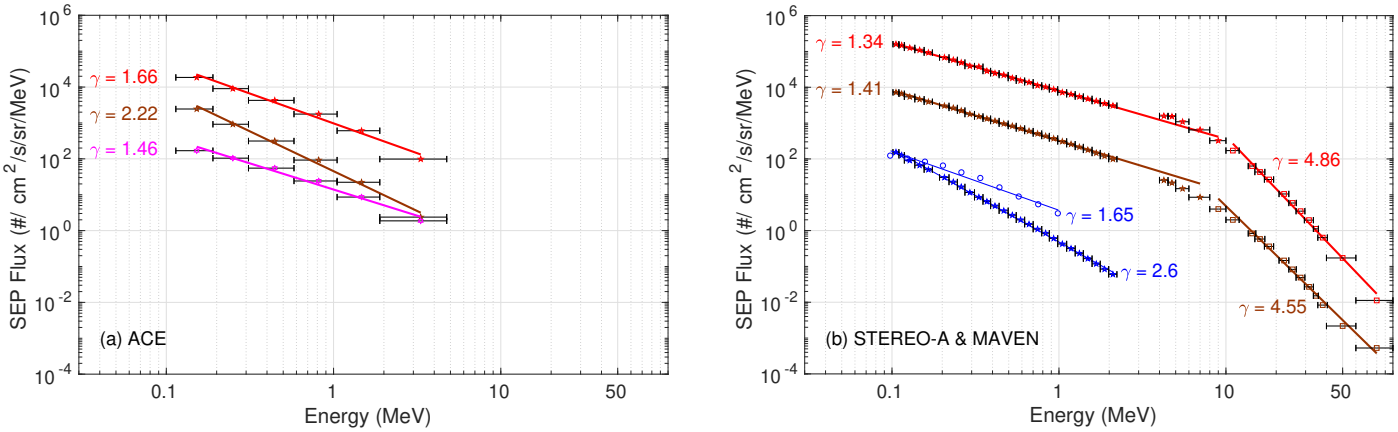

Figure 7. Power-law fits for (a) ACE, (b) STEREO-A and MAVEN observations of SEP events during July 2017. The left panel shows ACE observations during SEP periods from 14 to 17 July (red), 17 to 20 July (brown). The shock connected event from 27 to 30 July (magenta) is also shown. The right panel shows STEREO-A observations during SEP periods from 23 to 25 July (red), 25 to 27 July (brown). The SEP enhancements due to SIR event at STEREO-A (blue stars, 17 to 18 July) and MAVEN (blue circles, 14 to 17 July) are also shown.

Figure 7b shows the STEREO-A and MAVEN observed event averaged energy spectra during the SEP events of July 2017. There were two distinct SEP enhancements from 23 to 27 July, associated with CME eruptions. The spectra of these individual SEP events are shown in red (23/07, 10:48 UT to 25/07, 03:07 UT) and brown (25/07, 05:31 UT to 27/07, 23:16 UT) colors. The energy spectra are fitted with a double power law characterized by a spectral break at few tens of MeV. The spectral transition (or break) is observed between 6 and 10 MeV energy. A double power law or a power law with exponential rollover at a few to tens of MeV has been reported in many events (e.g., Zhao, Zhang, and Rassoul (2016)). The blue color fits shows the event averaged energy spectra for the 17 July SIR event observed by STEREO-A at ∼0.96 au (17/07, 00:00 UT to 18/07, 09:50 UT) and MAVEN at ∼1.58 au (14/07, 18:00 UT to 17/07, 13:12 UT). As mentioned earlier, the longitudinal separation between MAVEN and STEREO-A was about 46°, with the stream arriving at MAVEN before STEREO-A. The event averaged energy spectra of the CME event observed by MAVEN is not shown here due to the electron contamination to the ion channels.

The spectral analysis shows that the STEREO-A and Mars directed SEP events associated with the 25 July interplanetary CME are stronger (spectral indices of 1.3 and 1.4) than the Earth directed SEP events associated with the 16 July interplanetary CME (indices of 1.6 and 2.2). Also, the peak intensities are higher by around an order of magnitude for the 25 July event. The SEP event due to shock connectivity observed at Earth between 28 and 30 July is having a spectral index of 1.4 which is similar to the index of the 25 to 27 July event directly seen by STEREO-A. An onset delay of ∼2 days is observed for the shock connected event, which is due to the separation between the shock and observer location.

The 17 July SIR event observed at MAVEN and STEREO-A is having spectral indices of 1.6 and 2.6 respectively. Enhanced particle intensities by a factor of 6 (for 1 MeV ions) are observed at Mars, also the event spectrum is harder, indicating acceleration of energetic ions during the radial propagation of ∼0.62 au.

4 Discussion

The onset time of the CME event at a location can be calculated using Velocity Dispersion Analysis (VDA), which is based on the assumptions that the first particles observed at a given distance from the Sun have been released simultaneously, propagate the same path length, and experience no scattering or energy changes (Laitinen, Huttunen-Heikinmaa, Valtonen, & Dalla, 2015). According to this, the CME event onset time,

$$t_{onset}(v) = t_{injection} + (s/v) \ ,$$

where $t_{injection}$ is the particles' injection time at the source, s is the traveled distance, and v is the particle velocity. The injection of particles starts during the CME eruption from the Sun. For the 16 July CME event (Earth directed), eruption starts at ∼01:25 UT on 14 July (Figure 2a, `https://cdaw.gsfc.nasa.gov/CME_list/`), the particles with a speed of 664 km sec^{-1} will arrive at 0.99 au [ACE location] in ∼62 hours. For the 25 July CME event (STEREO-A and Mars directed), the injection starts at ∼04:54 UT on 23 July (Figure 2b, `http://spaceweather.gmu.edu/seeds/secchi.php`), the particles released with a speed of 811 km sec^{-1} will arrive at 0.96 au [STEREO-A location] in ∼49 hours, while the particles will arrive at 1.58 au [MAVEN location] in ∼81 hours. These calculations of event arrival times are matching with the observations of CME arrival at ACE (Figure 4), STEREO-A and Mars (Figures 5 and 6).

The context and space weather impacts of September 2017 solar events are extensively studied for Earth as well as for Mars (Jiggens et al., 2019; Lee et al., 2018; Liu, Zhu, & Zhao, 2019). Both July and September solar and SEP events had similar characteristics due to similar source region and eruptions (Luhmann et al., 2018). The spectral indices of the 4, 6, and 10 September SEP events are 0.5, 1.3, and 1.2 respectively for ACE observations (Bruno et al., 2019). While the spectral indices of 14 to 20 July events are 1.6 and 2.2 (Figure 7a). The spectral indices of the 4, 10, and 17 September SEP events are 0.2, 1.2, and 1.2 respectively for STEREO-A observations (Bruno et al., 2019). While the spectral indices of 23 to 27 July events are 1.3 and 1.4 (Figure 7b). Thus the Earth directed events of July was softer compared to the Earth directed events of September, while the STEREO-A directed events of July and September are of similar spectral characteristics.

As mentioned earlier, for the SIR event observations at STEREO-A and Mars, enhanced particle intensities are observed by MAVEN. Also the event averaged spectrum is more harder at Mars (Figure 7b), indicating acceleration of energetic ions during the radial propagation of ∼0.62 au. Similar particle flux enhancements associated with CIR events near 1.5 au are reported previously by Thampi, Krishnaprasad, Shreedevi, Pant, and Bhardwaj (2019). The observations of SEP events during CMEs suggests that shock acceleration takes place within 1 au itself during CME events (Thampi et al., 2019). The observations of SIR related SEP enhancements observed near Mars compared to 1 au are important in this context because of the addition of a vantage point at 1.5 au, and as such observations were previously sparse between 1 and 3 au.

5 Conclusions

The solar events of July 2017 are studied using observations from multiple spacecraft near Earth, near Mars, and STEREO-A. The three heliolongitude observations, along with the radial gradient between Earth and Mars provides an opportunity to study both longitudinal and radial variation of SEPs propagating in the inner heliosphere. The STEREO-A was ∼125° separated from Earth, while Mars had an angular separation of ∼175° with respect to Earth. The widespread observations of energetic particles was associated with activity originated at AR 12665 located at WS07W44 on the Sun.

There were two major interplanetary CME events and one SIR event during July 2017. The 16 July CME was directed west of Earth and the 25 July CME was in the general direction of STEREO-A and Mars. Earth and Mars were on the opposite sides of the solar disk, while Mars and STEREO-A were aligned with respect to the nominal Parker field. The 25 July event had higher plasma velocities and around an order of magnitude higher SEP flux compared to the 16 July event, also the event was wider (>120°) in heliolongitude. This CME shock had magnetic connectivity to Earth, which produced an SEP event at Earth from 28 to 30 July (Luhmann et al., 2018). An onset delay of ∼2 days is observed for the event arrival at ACE location. The spectral indices of the SEP event observed directly at STEREO-A and remotely at ACE was found to be similar (∼1.4). The 17 July SIR event was observed by both MAVEN and STEREO-A. Higher particle intensities by a factor of 6 for 1 MeV ions, and spectral hardening from 2.6 to 1.6 are observed at 1.58 au, indicating an acceleration of energetic ions in SIR shock during the radial propagation of 0.62 au in the interplanetary space.

Acknowledgments

The work is supported by the Indian Space Research Organisation (ISRO). The MAVEN data used in this work are taken from the Planetary Data System (`https://pds.nasa.gov/`). We gratefully acknowledge the MAVEN team for the data. The ACE/EPAM data are taken from the ACE Science Center (`http://www.srl.caltech.edu/ACE/ASC/`). The STEREO-A/IMPACT SEP data are taken from STEREO Science Center at `http://www.srl.caltech.edu/STEREO/`. The SDO AIA images are from `https://sdo.gsfc.nasa.gov/`. The STEREO-A/SECCHI EUVI and COR2 images are from STEREO Science Center at `https://stereo-ssc.nascom.nasa.gov/`. The SOHO LASCO images are from `https://soho.nascom.nasa.gov/`. The solar wind velocity and IMF near 1 au as well as the GOES SEP flux data are obtained from the SPDF OMNIWeb data center (`https://omniweb.gsfc.nasa.gov/`). We thank the staff of the ACE and STEREO Science Centers for providing the ACE and STEREO data and OMNIWeb team for providing the interplanetary and GOES data. The WSA-ENLIL+Cone model simulations are provided by CCMC through their public Runs on Request system (`https://ccmc.gsfc.nasa.gov/`). We thank M. L. Mays, CCMC, NASA GSFC for their public model runs. C. Krishnaprasad acknowledges the financial assistance provided by ISRO through a research fellowship. This research has made use of SunPy v1.1, an open-source and free community-developed solar data analysis Python package (`https://sunpy.org/`).

References

Bruno, A., Christian, E. R., de Nolfo, G. A., Richardson, I. G., & Ryan, J. M. (2019). Spectral analysis of the September 2017 Solar Energetic Particle Events. *Space Weather*, *17*(3), 419-437. doi: 10.1029/2018SW002085

Cane, H. V., Reames, D. V., & von Rosenvinge, T. T. (1988). The role of interplanetary shocks in the longitude distribution of solar energetic particles. *Journal of Geophysical Research*, *93*(A9), 9555-9567. doi: 10.1029/JA093iA09p09555

Chollet, E. E., Mewaldt, R. A., Cummings, A. C., Gosling, J. T., Haggerty, D. K., Hu, Q., ... Sauvaud, J.-A. (2010). Multipoint connectivity analysis of the May 2007 solar energetic particle events. *Journal of Geophysical Research: Space Physics*, *115*(A12). doi: 10.1029/2010JA015552

Desai, M., & Giacalone, J. (2016). Large gradual solar energetic particle events. *Living Reviews in Solar Physics*, *13*(1), 3. doi: 10.1007/s41116-016-0002-5

Dumbović, M., Guo, J., Temmer, M., Mays, M. L., Veronig, A., Heinemann, S. G., ... Wimmer–Schweingruber, R. F. (2019). Unusual plasma and particle signatures at Mars and STEREO-A related to CME–CME interaction. *The Astrophysical Journal*, *880*(1), 18. doi: 10.3847/1538-4357/ab27ca

Gold, R., Krimigis, S., Hawkins, S., Haggerty, D., Lohr, D., Fiore, E., ... Lanzerotti, L.

(1998). Electron, Proton, and Alpha Monitor on the Advanced Composition Explorer spacecraft. *Space Science Reviews*, *86*(1), 541–562. doi: 10.1023/A:1005088115759

Halekas, J. S., Ruhunusiri, S., Harada, Y., Collinson, G., Mitchell, D. L., Mazelle, C., ... Jakosky, B. M. (2017). Structure, dynamics, and seasonal variability of the Mars-solar wind interaction: MAVEN Solar Wind Ion Analyzer in-flight performance and science results. *Journal of Geophysical Research: Space Physics*, *122*(1), 547-578. doi: 10.1002/2016JA023167

Jiggens, P., Clavie, C., Evans, H., O'Brien, T. P., Witasse, O., Mishev, A. L., ... Nagatsuma, T. (2019). In Situ Data and Effect Correlation During September 2017 Solar Particle Event. *Space Weather*, *17*(1), 99-117. doi: 10.1029/2018SW001936

Klein, K.-L., & Dalla, S. (2017). Acceleration and Propagation of Solar Energetic Particles. *Space Science Reviews*, *212*(3), 1107–1136. doi: 10.1007/s11214-017-0382-4

Krishnaprasad, C., Thampi, S. V., & Bhardwaj, A. (2019). On the response of Martian Ionosphere to the Passage of a Corotating Interaction Region: MAVEN Observations. *Journal of Geophysical Research: Space Physics*, *124*(8), 6998-7012. doi: 10.1029/2019JA026750

Laitinen, T., Huttunen-Heikinmaa, K., Valtonen, E., & Dalla, S. (2015). Correcting for interplanetary scattering in velocity dispersion analysis of solar energetic particles. *The Astrophysical Journal*, *806*(1), 114. doi: 10.1088/0004-637x/806/1/114

Larson, D. E., Lillis, R. J., Lee, C. O., Dunn, P. A., Hatch, K., Robinson, M., ... Jakosky, B. M. (2015). The MAVEN Solar Energetic Particle Investigation. *Space Science Reviews*, *195*(1), 153–172. doi: 10.1007/s11214-015-0218-z

Lee, C. O., Jakosky, B. M., Luhmann, J. G., Brain, D. A., Mays, M. L., Hassler, D. M., ... Halekas, J. S. (2018). Observations and Impacts of the 10 September 2017 Solar Events at Mars: An Overview and Synthesis of the Initial Results. *Geophysical Research Letters*, *45*(17), 8871-8885. doi: 10.1029/2018GL079162

Liu, Y. D., Zhu, B., & Zhao, X. (2019). Geometry, Kinematics, and Heliospheric Impact of a Large CME-driven Shock in 2017 September. *The Astrophysical Journal*, *871*(1), 8. doi: 10.3847/1538-4357/aaf425

Luhmann, J. G., Mays, M. L., Li, Y., Lee, C. O., Bain, H., Odstrcil, D., ... Petrie, G. (2018). Shock Connectivity and the Late Cycle 24 Solar Energetic Particle Events in July and September 2017. *Space Weather*, *16*(5), 557-568. doi: 10.1029/2018SW001860

Mays, M. L., Taktakishvili, A., Pulkkinen, A., MacNeice, P. J., Rastätter, L., Odstrcil, D., ... Kuznetsova, M. M. (2015). Ensemble Modeling of CMEs Using the WSA–ENLIL+Cone Model. *Solar Physics*, *290*(6), 1775–1814. doi: 10.1007/s11207-015-0692-1

Mewaldt, R. A., Cohen, C. M. S., Cook, W. R., Cummings, A. C., Davis, A. J., Geier, S., ... Wortman, K. (2008). The Low-Energy Telescope (LET) and SEP Central Electronics for the STEREO Mission. *Space Science Reviews*, *136*(1), 285–362. doi: 10.1007/s11214-007-9288-x

Müller-Mellin, R., Böttcher, S., Falenski, J., Rode, E., Duvet, L., Sanderson, T., ... Smit, H. (2008). The Solar Electron and Proton Telescope for the STEREO Mission. *Space Science Reviews*, *136*(1), 363–389. doi: 10.1007/s11214-007-9204-4

Odstrcil, D. (2003). Modeling 3-D solar wind structure. *Advances in Space Research*, *32*(4), 497 - 506. (Heliosphere at Solar Maximum) doi: 10.1016/S0273-1177(03)00332-6

Parker, E. N. (1958). Dynamics of the Interplanetary Gas and Magnetic Fields. *The Astrophysical Journal*, *128*, 664. doi: 10.1086/146579

Rahmati, A., Larson, D. E., Cravens, T. E., Lillis, R. J., Dunn, P. A., Halekas, J. S., ... Jakosky, B. M. (2015). MAVEN insights into oxygen pickup ions at Mars. *Geophysical Research Letters*, *42*(21), 8870-8876. doi: 10.1002/2015GL065262

Reames, D. V. (1995). Solar energetic particles: A paradigm shift. *Reviews of Geophysics*, *33*(S1), 585–589. doi: 10.1029/95RG00188

Reames, D. V. (2013). The two sources of solar energetic particles. *Space Science Reviews*, *175*(1), 53–92. doi: 10.1007/s11214-013-9958-9

Richardson, I. G., von Rosenvinge, T. T., Cane, H. V., Christian, E. R., Cohen, C. M. S.,

Labrador, A. W., ... Stone, E. C. (2014). >25 MeV Proton Events Observed by the High Energy Telescopes on the STEREO A and B Spacecraft and/or at Earth During the First Seven Years of the STEREO Mission. *Solar Physics*, *289*(8), 3059–3107. doi: 10.1007/s11207-014-0524-8

Thampi, S. V., Krishnaprasad, C., Bhardwaj, A., Lee, Y., Choudhary, R. K., & Pant, T. K. (2018). MAVEN observations of the response of Martian ionosphere to the interplanetary coronal mass ejections of March 2015. *Journal of Geophysical Research: Space Physics*, *123*(ja), 6917 - 6929. doi: 10.1029/2018JA025444

Thampi, S. V., Krishnaprasad, C., Shreedevi, P. R., Pant, T. K., & Bhardwaj, A. (2019). Acceleration of Energetic Ions in Corotating Interaction Region near 1.5 au: Evidence from MAVEN. *The Astrophysical Journal Letters*, *880*(1), L3. doi: 10.3847/2041-8213/ab2b43

Van Hollebeke, M. A. I., Ma Sung, L. S., & McDonald, F. B. (1975). The Variation of Solar Proton Energy Spectra and Size Distribution with Heliolongitude. *Solar Physics*, *41*(1), 189-223. doi: 10.1007/BF00152967

von Rosenvinge, T. T., Reames, D. V., Baker, R., Hawk, J., Nolan, J. T., Ryan, L., ... Wiedenbeck, M. E. (2008). The High Energy Telescope for STEREO. *Space Science Reviews*, *136*(1), 391–435. doi: 10.1007/s11214-007-9300-5

von Rosenvinge, T. T., Richardson, I. G., Reames, D. V., Cohen, C. M. S., Cummings, A. C., Leske, R. A., ... Wiedenbeck, M. E. (2009). The solar energetic particle event of 14 December 2006. *Solar Physics*, *256*(1), 443–462. doi: 10.1007/s11207-009-9353-6

Xie, H., Mäkelä, P., St. Cyr, O. C., & Gopalswamy, N. (2017). Comparison of the coronal mass ejection shock acceleration of three widespread SEP events during solar cycle 24. *Journal of Geophysical Research: Space Physics*, *122*(7), 7021-7041. doi: 10.1002/2017JA024218

Zhang, M., Qin, G., & Rassoul, H. (2009). Propagation of solar energetic particles in three-dimensional interplanetary magnetic fields. *The Astrophysical Journal*, *692*(1), 109–132. doi: 10.1088/0004-637x/692/1/109

Zhao, L., Zhang, M., & Rassoul, H. K. (2016). Double power laws in the event-integrated solar energetic particle spectrum. *The Astrophysical Journal*, *821*(1), 62. doi: 10.3847/0004-637X/821/1/62